Available online at www.sciencedirect.com
SCIENCE DIRECT®
Surface & Coatings Technology 200 (2006) 6047 – 6053
SURFACE & COATINGS TECHNOLOGY
www.elsevier.com/locate/surfcoat

# Growth of $CrN_x$ films by DC reactive magnetron sputtering at constant $N_2$/Ar gas flow

E. Forniés, R. Escobar Galindo, O. Sánchez, J.M. Albella*

*Instituto de Ciencia de Materiales de Madrid (CSIC), 28049 Cantoblanco, Madrid, Spain*

Received 11 March 2005; accepted in revised form 18 September 2005
Available online 2 November 2005

**Abstract**

Chromium nitride coatings have been deposited on silicon by magnetron sputtering in an $Ar+N_2$ atmosphere at different bias substrate voltages. The poisoning effect has been studied monitoring the discharge voltage and total pressure. The chemical composition and crystalline structure have been analysed by Glow Discharge Optical Emission Spectroscopy (GDOES) and X-ray Diffraction (XRD), respectively. Changing simultaneously the relative $N_2$ ($f_{N2}$) and Ar ($f_{Ar}$) flow rates, while keeping constant the total gas flow (at 11sccm), different crystalline phases are observed. At low $N_2$ concentrations, $f_{N2}<2\%$, pure Cr is detected. At increasing $N_2$ flow rates ($5\%<f_{N2}<40\%$) the following sequence of phases is found: [Cr+N], [Cr+$CrN_x$] and [Cr+CrN]. Finally, in the range $50\%<f_{N2}<100\%$ only the hexagonal phase $Cr_2N$ is obtained. Scanning electron microscopy (SEM) has been used to obtain the microstructure, revealing that it changes from columnar to granular when the substrate bias varies in the range from +20 V to −150 V. Nanoindentation and pin-on-disk experiments have been also carried out to correlate the tribological behaviour of the coatings with the observed crystalline phases.
© 2005 Elsevier B.V. All rights reserved.

*Keywords:* CrN; Sputtering; Hardness; Bias; GDOES; Pin-on-disk

## 1. Introduction

In the last decades, transition metal nitride coatings have attracted the interest of many laboratories due to their outstanding mechanical and tribological properties: high hardness (20–25 GPa, approximately), good adhesion to metal substrates, high critical load, and relatively good corrosion and wear resistance. They also present metallic lustre, and for these reasons the coatings are mainly used as protective layers for machinery components and tools as well as decorative coatings. Among them, $TiN_x$ and $CrN_x$ deposited by reactive magnetron sputtering and cathodic arc techniques have been the subject of more intensive research for hard coating applications. Despite its better properties, such as oxidation and corrosion resistance [1–5], microhardness, toughness [6] and wear resistance [7] $CrN_x$ has been less studied than $TiN_x$ coatings.

Focusing on the $CrN_x$ deposition by reactive magnetron sputtering, different phases, depending on the nitrogen flow rate, can be obtained: Cr, Cr+N, Cr+N+$Cr_2N$, $Cr_2N$+CrN, CrN [8–16]. The composition of the $CrN_x$ coatings is strongly determined by different processes, which take place both at the cathode and sample surface during the sputtering process [17–20]. All these processes are determined by the discharge parameters, namely voltage and intensity, relative Ar/$N_2$ flow rate, pressure, pumping rate, etc.

As it is well known, at low $N_2$ flow rates most of the nitrogen molecules are gettered by the sputtered Cr atoms coming from the target and then deposited on the substrate and chamber walls. In this case, the concentration of Ar atoms in the chamber is high enough to keep the target as pure Cr, and the coating is mainly composed by a mixture of chromium and gettered molecules. When the $N_2$ flow is increased, a critical range is reached where the excess of nitrogen gas in the chamber starts to react with the target surface [17]. In this situation, the gas mixture induces two competitive effects on the target surface: the reacted nitrogen provokes the formation of a Cr–N layer partially covering the target surface while Ar ions impinging on the target remove this Cr–N layer. The balance between these two processes determines the relative phase composition of the

* Corresponding author.
*E-mail address:* jmalbella@icmm.csic.es (J.M. Albella).

0257-8972/$ - see front matter © 2005 Elsevier B.V. All rights reserved.
doi:10.1016/j.surfcoat.2005.09.020

coatings (i.e., sputtered chromium + $CrN_x$ compounds). Above this range, the formation rate of the Cr–N layer becomes higher than its sputtering rate, and the target is said to be poisoned [17,19,20]. The exact coating composition then is strongly related to the Cr–N layer formed on the target and, in a lesser extent, to the gettered species.

However, the interplay between the different plasma parameters controlling the target poisoning and the $CrN_x$ phases is still not well understood. To our knowledge, most of the authors have studied the reactive gas flow influence at constant Ar flow, varying the $N_2$ flow in the chamber. Under these conditions, the stoichiometric CrN phase is generally obtained [8,9,11–15]. In these experiments, the discharge pressure may vary widely and, besides, this method largely limits the available range of $N_2$/Ar proportions. So, in order to get further insight into the deposition mechanisms in a wide range of $N_2$/Ar ratios, we have kept constant the total gas flow ($f_{tot}$) while changing both partial flow rates, thus allowing us to sweep a wide range of processes, from pure Ar to pure $N_2$. We have studied the phase formation, composition, microstructure, deposition rate and tribological properties of $CrN_x$ coatings at different $N_2$/Ar gas ratios (from 0 to 1). The influence of the bias voltage on the mentioned properties has been also investigated in this paper.

## 2. Experimental

The chromium nitride coatings were deposited on single-crystal Si(100) wafers by DC planar magnetron sputtering. It consists of a circular planar cathode, 7.5 cm in diameter, placed in front of the substrate holder, at a distance of 6.5 cm. The base pressure of the chamber was $2 \cdot 10^{-4}$ Pa approximately and the working pressure was in the range 0.16–0.23 Pa. During the deposition process the substrate temperature was monitored with a thermocouple located on the back of the holder plate. Other details of the sputtering system have been described previously [21].

The coatings used to study the bias influence were deposited with an interlayer of Cr, 338 nm thick, to improve the adherence. In all the experiments, the cathode power was held constant at 100 W. Positive and negative bias voltages (+20 V, 0 V, −50 V, −100 V and −150 V) were applied to the substrate holder by a DC power supply. In the case of the coatings with Cr interlayer, no bias was applied during the interlayer growth. No intentional heating was made, though the process temperature of the substrates was relatively constant at 90–100 °C.

Prior to deposition, 20 min of presputtering was performed in order to remove the metal-nitride layer of the cathode due to previous deposits. The chromium target used is a commercial target of purity 99.95%. A mixture of Ar (99.999%) and $N_2$ (99.9992%) gases was introduced in the vacuum chamber. The $N_2$ relative flow rate ($f_{N2}$) was varied from 2% to 100% of the total flow rate ($f_{tot}$ = 11 sccm) by changing simultaneously both Ar and $N_2$ flow rates.

Crystalline structure was determined by a D8 diffractometer with Bragg–Brentano geometry using $CuK_\alpha$ radiation. The morphology of the coatings was characterised by Scanning Electron Microscopy, SEM (Hitachi S-2700). The chemical composition of the films was determined by Rutherford Backscattering Spectroscopy, RBS, in a Van der Graaff accelerator of 2 MeV and by rf-Glow Discharge Optical Emission Spectroscopy, rf-GDOES (Jobin Yvon GD-profiler). The rf-GDOES set-up was calibrated using certified standards and $CrN_x$ coatings measured by RBS. The thickness was measured using a stylus profilometer (Dektak 3030).

Wear resistance was determined by pin-on-disk using as counterpart a WC/Co ball of 1.5 mm radii. Test parameters were: wear track 2 mm diameter, normal load 3 N and rotation speed 300 rev/min. Hardness ($H$) was determined by a Berkovich indenter (Micromaterials). The measurements were made at different load ranges between 1–3 mN, 3–10 mN and 10–50 mN.

## 3. Results and discussion

### 3.1. Influence of $N_2$ flow rate

Figs. 1 and 2 show the X-ray diffraction diagrams of the coatings obtained at increasing $N_2$ flows ($f_{N2}$) from 0 to 11 sccm, while reducing the Ar flow ($f_{Ar}$) in the same proportion to keep $f_{tot}$ constant. As can be appreciated, at $f_{N2}$ = 2% the only phase present in the coatings is pure chromium, identified in the diffraction diagram by the peak Cr(110) at 44.39°. However, at higher nitrogen flows the nitrogen starts to incorporate into the coating as it has been detected by the rf-GDOES (see Fig. 3a). The insertion of nitrogen causes an increase of non-uniform stresses as well as the formation of different $CrN_x$ phases, provoking the broadening and a small shift of the main peak at about 44° [12].

In the diffraction diagrams of Fig. 1, between $f_{N2}$ = 5% and 30%, the main peak evolves approaching to the CrN(200) peak at 43.774°, though it is not possible to ascertain the presence of this phase in this flow range. However, at the relative nitrogen flow of 40% CrN(200), CrN(220), CrN(111), and CrN(311)

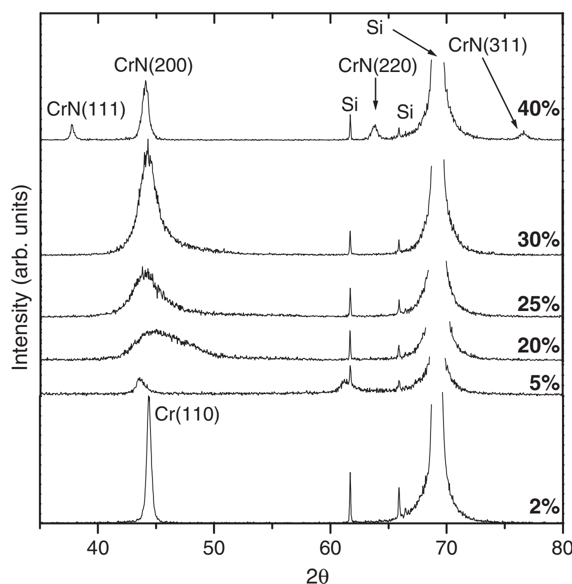


Fig. 1. XRD diagrams of $f_{N2}$ from 2% to 40%.

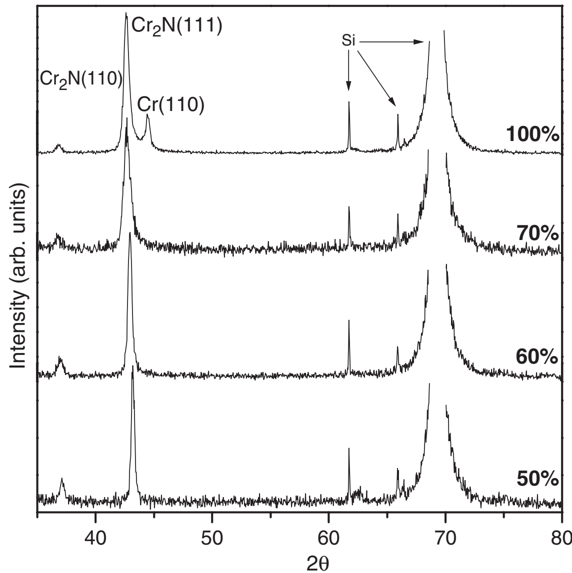


Fig. 2. XRD diagrams of $f_{N2}$ from 50% to 100%.

peaks are already identified in the X-ray spectra. Nevertheless, the results obtained by rf-GDOES indicate that nitrogen concentration in the films at this flow rate is 36%, clearly below the concentration corresponding to stoichiometric CrN. Thus, although the only phase present is the cubic CrN, there is an excess of chromium in the films, which is not detected in the diffraction diagram. Hence, the excess of Cr is supposed to be incorporated in amorphous form or as interstitial atoms in the CrN lattice.

For $f_{N2}$ = 50–100%, the peaks CrN(220) and CrN(311) are not present anymore as can be seen in Fig. 2. Thus, in the abovementioned range only two peaks, $Cr_2N$(111)-42.61° and $Cr_2N$(110)-37.35° are detected, except in the case of $f_{N2}$ = 100% where the Cr(110)-44.39° peak is also detected, because this sample was deposited with a 338 nm thick chromium interlayer. These results indicate a phase transition, from cubic CrN to hexagonal $Cr_2N$, approximately between $f_{N2}$ = 40% and 50%. This is in contrasts to other authors who found the CrN phase at the highest $N_2$ flows [8,9,11–16].

Rf-GDOES measurements (Fig. 3a) show two clear regions: (1) below $f_{N2}$ = 40%, characterised by a linear increase of the N concentration, and (2) above 40%, where the incorporation of N is constant at a value of 36% approximately. Similar results have been obtained elsewhere but with different values of the nitrogen saturation [13,22]. Besides, above $f_{N2}$ = 40% only the single $Cr_2N$ phase is formed, even in the case where $N_2$ is used as working and reactive gas. We have performed some experiments with a total flow of 25 sccm of $N_2$ that yielded to the same results.

The saturation of nitrogen incorporation into the coating should induce a change in total pressure ($P_{tot}$). In Fig. 3a (right *y* axis), the $P_{tot}$ values measured for increasing $f_{N2}$ flows are represented. We can observe again two different regimes, below and above $f_{N2}$ = 40%. In both cases there is a linear decrease of $P_{tot}$ with $f_{N2}$, but in the former one the slope is 3.14 times higher (in absolute values) than in the latter. In order to clarify this point we have compared in Fig. 3b the variation of the total pressure versus $f_{N2}$ during the process (i.e., with discharge) and without discharge. When no process is taking place there is a linear decrease of the $P_{tot}$ which is explained by the higher pumping speed of $N_2$ than that of Ar [23]. When the discharge is on, there is also a linear decrease of the $P_{tot}$, with a similar slope than without discharge, but approximately 0.01 Pa below. The difference between both lines corresponds with the incorporation of nitrogen into the coating and into the chamber walls.

For $f_{N2}$ flows above 40% the slope of the $P_{tot}$ curve, with discharge, changes to higher values than in the former regime, while without discharge, the slope keeps constant. The change in $P_{tot}$ slope can be explained by the target poisoning. As it is known, the sputtering rate from a poisoned target is lower than that of pure metallic target [19,20], and therefore less metal atoms and less reactive gas are consumed. This effect, combined with the higher temperature of the chamber (60 °C approximately), induces the observed slower decrease of $P_{tot}$ with discharge even up to higher values than those without discharge (see the experimental dot at 100% in Fig. 3b).

Target poisoning can also be detectable by the analysis of the discharge voltage. The power has been, in all the experiments,

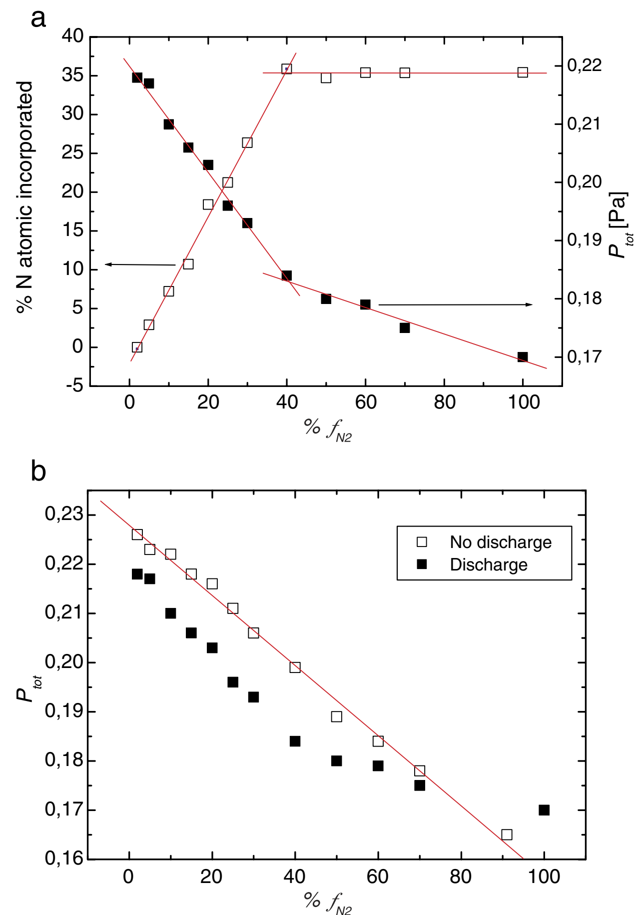


Fig. 3. (a) (above): N concentration into the coating measured by rf-GDOES (left *y* axis) and the total pressure (right *y* axis) as a function of $f_{N2}$. (b) (below): Total pressure ($P_{tot}$) with discharge (closed symbols) and without discharged (open symbols) as a function of $f_{N2}$.

kept constant at 100 W. As a result of the target nitridation the yield of Cr atoms sputtered from the nitrided surface is reduced. Several effects contribute to the increase of the discharge voltage. On the one hand, the lower ionisation probability of nitrogen, as compared to that of argon, increases the plasma impedance when $f_{N2}$ increases, and hence, the discharge voltage [17]. On the other hand, the different Secondary-Electron Emission Coefficient (SEEC) of a metal and its nitride is well known. Mientus et al. [18] obtained, for chromium target and nitrogen as reactive gas, an upraising of the voltage with the nitrogen partial pressure, suggesting a lower SEEC of chromium nitride than that of pure chromium.

To check the influence of these two effects, we have represented in Fig. 4 the variation of the discharge voltage versus deposition time for different $f_{N2}$. Every single process begins with a presputtering in Ar in order to remove nitride layer from the target surface. The discharge voltage of every process increases with increasing $f_{N2}$ indicating a higher discharge impedance as a consequence of the lower ionisation probability of $N_2$ than that of Ar. Processes at $f_{N2}$=30% and 35% are revealed when the poisoning is showing up. For $f_{N2}$=30%, the voltage shows a slow increase until 30 min of process, where it remains constant. This raising tendency also happens at $f_{N2}$=35%, but at lower deposition times due to the higher flow of $N_2$. For $f_{N2} \geq 40\%$ the target poisoning takes place at the beginning of the process (approximately in the first 10 min). Since the gas flow is constant, the voltage increase must be produced by the poisoning of the target, indicating that chromium nitride has a lower SEEC than that of Cr, in agreement with Mientus et al. [18]. In parallel with these experiments, we have observed a decrease of the deposition rate, $R$, from 24 nm/min to 11 nm/min with increasing $f_{N2}$, which is explained by the lower sputter efficiency of $N_2$ than that of Ar along with the poisoning effect provoked by nitrogen incorporation into the target [24].

### 3.2. Influence of the substrate bias

To study the influence of the bias, the nitrogen relative flows have been fixed at 40% and 70%, where the two $CrN_x$ phases (CrN, $Cr_2N$) have been detected. Different bias voltages (+20 V, 0 V, −50 V, −100 V, −150 V) were applied to the substrates during deposition process in order to know its influence on the structure of the films. A first group of coatings grown on silicon was deposited without any metal interlayer using a bias voltage. However, some of these coatings deposited at high negative bias flaked, and those that did not flake presented cracks after performing the pin-on-disk tests. In this case, the higher the N incorporation and the absolute values of the negative bias were, the worse the results in terms of adherence were. Therefore, in order to improve the adherence and reduce the residual stress [8,25], a second group of coatings was deposited on silicon with a 338 nm thick interlayer of chromium, as indicated in Table 1. All the coatings of this group presented good adhesion.

Table 1
Sample identification and summary of the bias effect

| Sample | $\%f_{N2}$ | $\%N_{inc}$ | $P_{tot}$ [$10^{-3}$ mb] | Bias [V] | Thickness $CrN_x$ [nm] | $R$ [nm/min] |
|---|---|---|---|---|---|---|
| CrN58 | 40 | 30.64 | 1.96 | +20 | 1150 | 19.17 |
| CrN51 | | 41.21 | 1.96 | 0 | 1092 | 18.20 |
| CrN52 | | 32.93 | 1.84 | −50 | 1150 | 19.17 |
| CrN53 | | 37.98 | 2.11 | −100 | 1415 | 15.03 |
| CrN54 | | 23.62 | 1.91 | −150 | 1092 | 11.01 |
| CrN59 | 70 | 43.15 | 1.73 | +20 | 757 | 12.62 |
| CrN46 | | 32.44 | 1.67 | 0 | 752 | 13.03 |
| CrN55 | | 36.11 | 1.69 | −50 | 789 | 12.53 |
| CrN56 | | 36.98 | 1.70 | −100 | 600 | 10.00 |
| CrN57 | | 43.32 | 1.68 | −150 | 585 | 9.75 |

When the deposition process is carried out with a negative bias, the positive ions of the plasma ($Ar^+$, $N^+$ and $N_2^+$) are attracted towards the substrate holder, transferring their kinetic energy to the surface atoms. If the incident ion energy (higher with increasing negative bias) is high enough, this effect may induce a re-sputtering of the coating, giving rise to a lower deposition rate as can be clearly seen in Fig. 5. These results are in agreement with those obtained by Hurkmans et al. [1]. Besides the bias effect, the target poisoning is also apparent in Fig. 5, since the deposition rate values at $f_{N2}$=70% are much lower than at $f_{N2}$=40%.

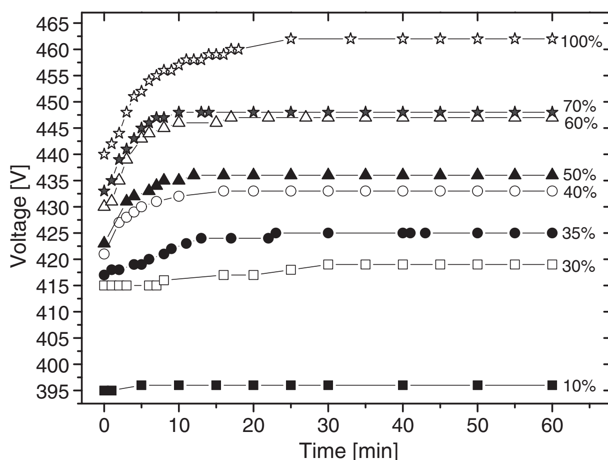


Fig. 4. Discharge voltage versus process time for different $N_2$ relative flows.

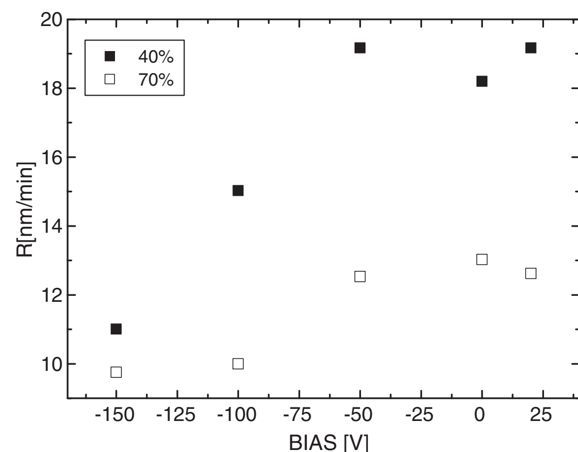


Fig. 5. Deposition rate at different bias for $f_{N2}$=40% and 70%.

By increasing the absolute values of the negative bias, the transferred energy increases the mobility of the adatoms on the coating surface and consequently denser coatings can be formed [26], at the expense of higher residual stresses [12,27]. On the contrary, positive bias results in the formation of a positive shield situated in the substrate holder that repels the positive ions and attracts the electrons present in the plasma, changing the situation from ion bombardment process to electron bombardment process [28]. As a consequence, the coating presents less residual stresses. This is shown in Table 2 for $f_{N2}=40\%$, where the theoretical ($a_{th}$) and experimental ($a_{exp}$) lattice parameter of CrN films are compared. As can be appreciated, the deviation ($\Delta a$) of the experimental from theoretical values at +20 V is minimum. However grounded substrates shows a shift of the diffraction peaks to lower values indicating the presence of residual tensile stresses [10]. Further increase of the negative bias provokes a broadening of the peaks (presence of inhomogeneous residual stress) and a high decrease of their intensities (see Figs. 6 and 7 for −50 V).

When $f_{N2}=40\%$ (Fig. 6), the only phase detected is CrN. Thus, it seems that the bias does not have any influence on the phase formation, contrary to the observations in other works [11], though we have detected changes in the preferred orientation. Note that at +20 V, the main peak observed (at $2\theta=63.60°$) corresponds to CrN(220) planes while at 0 V bias, the main peak corresponds to CrN(200) planes.

For coatings deposited at $f_{N2}=70\%$, at +20 V and 0 V there is no deviation to lower values of the $Cr_2N(111)$ peak, as it is also observed for $Cr_2N(110)$ peak. A similar effect to that occurring at $f_{N2}=40\%$ and −50 V takes place for $f_{N2}=70\%$, where no chromium nitride peak has been detected at −50 V (Fig. 7).

For $f_{N2}=70\%$, no phase change is observed with the applied bias and all the peaks correspond to $Cr_2N$. Nevertheless changes in preferred orientations can be also noticed at different applied bias, as it occurs for $f_{N2}=40\%$. The main peak detected in diffraction diagrams at +20 V, 0 V and −150 V corresponds to $Cr_2N(111)$, while $Cr_2N(110)$ is predominant at −100 V. Identical results have been obtained for samples prepared at the same bias but without Cr interlayer (not shown here for brevity), so it seems to be a reproducible effect. Cunha et al. [26] also found no phase change with applied bias.

Differences in microstructure can be observed in SEM pictures of the coatings as depicted in Fig. 8. It is evident that the microstructure is affected by the applied bias. SEM images show that at positive and low negative voltages (+20 V, 0 V,

Table 2
Lattice parameter values ($a$) and $\Delta a=a_{exp}-a_{th}$ obtained from different observed XRD peaks

| | (111) $a$ [Å] | (200) $a$ [Å] | (220) $a$ [Å] | (311) $a$ [Å] | Mean values $a$ [Å]; $\Delta a$ [Å] |
|---|---|---|---|---|---|
| No Cr interlayer (no bias 0 V) | 4.125 | 4.110 | 4.127 | 4.124 | 4.121±0.007<br>−0.019±0.007 |
| With Cr interlayer (no bias 0 V) | 4.175 | 4.167 | – | 4.174 | 4.172±0.004<br>0.032±0.004 |
| With Cr interlayer (bias +20 V) | 4.137 | – | 4.138 | 4.142 | 4.139±0.002<br>−0.001±0.002 |

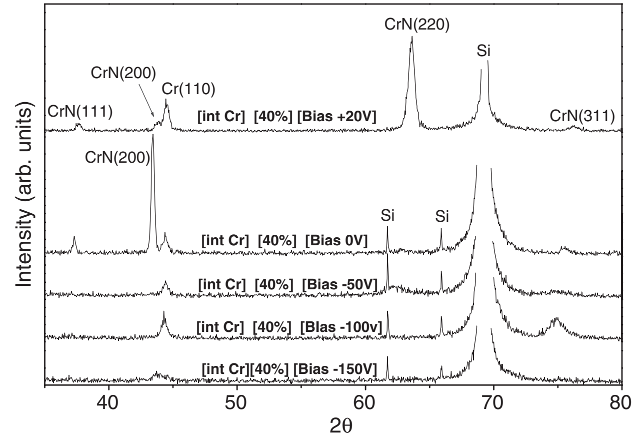


Fig. 6. XRD diagrams of $CrN_x$ coating obtained at different bias for $f_{N2}=40\%$ with a chromium interlayer.

−50 V) for both $f_{N2}=40\%$ and 70%, the coating grows with columnar structure, whereas at −100 V and −150 V, the microstructure changes to a granular structure. So it seems clear that at a voltage of −50 V a change in the growing process is taking place, shifting from columnar to granular structure.

### 3.3. Tribological results

Nanoindentation experiments were carried out on samples deposited in the whole range of $N_2$ flows. Due to the different thickness of the coatings, load considerations must be taken into account to give a precise hardness value. Preliminary measurements were carried out at different load regimens (from 1 mN to 50 mN). To avoid influences from the surface roughness, oxide layer [15] and chromium interlayer, the range from 3 mN to 10 nN was found to be valid for all the

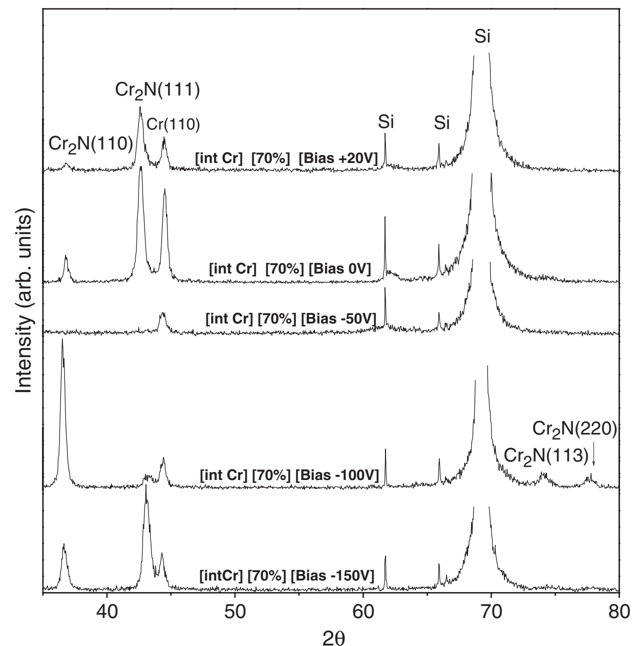


Fig. 7. XRD diagrams of $CrN_x$ coating obtained at different bias for $f_{N2}=70\%$ with a chromium interlayer.

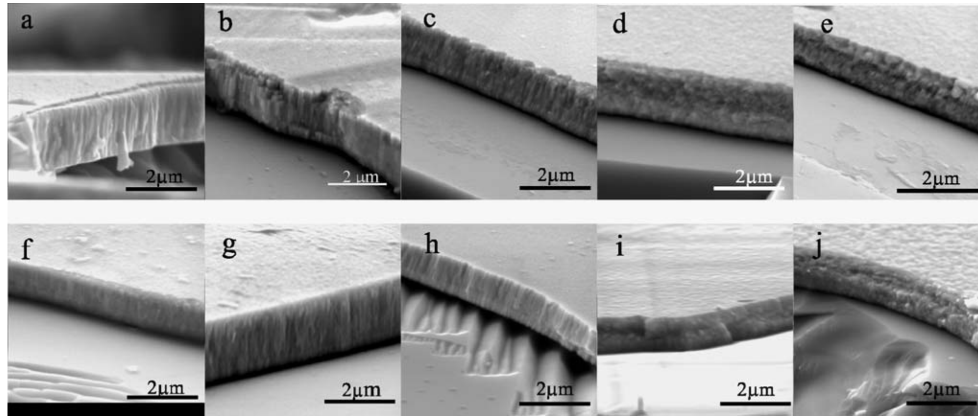


Fig. 8. SEM micrographs of different coatings deposited at different bias. First sequence of samples (a, b, c, d, e) were deposited applying voltages +20 V, 0 V, −50 V, −100 V, and −150 V respectively and $f_{N2}$=40%. Second sequence of samples (f, g, h, i, j) was deposited applying voltages +20 V, 0 V, −50 V, −100 V, and −150 V respectively and $f_{N2}$=70%.

samples. Several tests at variable loads (within this range) were made on different points of the surface coating. Hardness results (*H*) for the analysed coatings are shown in Fig. 9.

As can be observed, *H* values show a strong rise for $f_{N2}>2\%$, indicating that a small incorporation of nitrogen into the coating (7.2% according GDOES results) provokes a hardening of the coating up to 20 GPa, in accordance to the results found by other authors [11,29]. No clear tendency is observed above this value and the experimental error of the measurements does not allow asserting the influence of the different $CrN_x$ phases observed within this range. The hardness values, about 21 GPa, are quite similar to those found in the literature [8,10,11,13,16,29].

Regarding the influence of the bias, the hardness values versus applied bias for $f_{N2}$=70% and 40% have been represented in Fig. 10. It can be seen how the hardness of the samples deposited at $f_{N2}$=70% is higher in every case than those deposited at $f_{N2}$=40%. The excess of Cr atoms dispersed in the crystalline phase of the films deposited with $f_{N2}$=40%, may explain the lower hardness observed for the CrN films as compared to those deposited at $f_{N2}$=70% with the $Cr_2N$ structure. For both series, there is a certain trend of the hardness values to increase with negative bias, with a maximum value for the sample grown at $f_{N2}$=70% and −100 V bias ($H$=25±2 GPa). This trend can be explained by the more compact morphology of the coatings obtained for higher negative bias, as depicted by SEM micrographs (Fig. 8).

Pin-on-disk tests were also performed over the samples listed in Table 1. The volume loss has been calculated using the equation given by ASTM [30] assuming no significant pin wear. Fig. 11 presents the wear rate *K* given by the following equation:

$$K = \frac{V}{w \cdot s} \quad (1)$$

where *V* is the volume loss, *s* is the sliding distance and *w* is the normal load applied to the substrate (3 N). As can be appreciated, the bias exerts a strong influence on the wear rate for $f_{N2}$=70%, which shows a clear decrease with increasing negative bias. For coatings deposited at $f_{N2}$=40%, the wear rate seems not to be very influenced by the bias. It has been found a high dispersion in *K* for coating deposited at +20 V.

The presence of metallic Cr atoms in the crystalline phase of CrN matrix (samples grown at $f_{N2}$=40%), as stated above, is

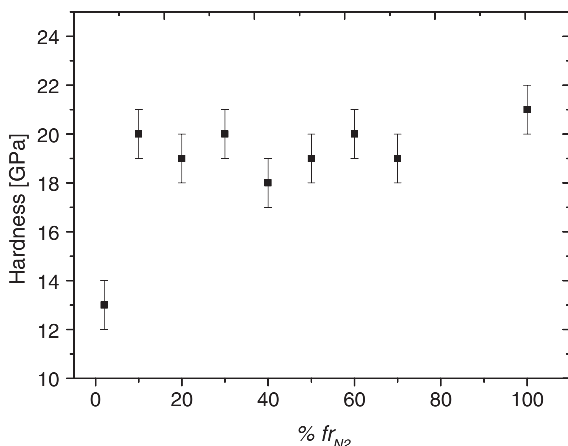


Fig. 9. Hardness values, measured with Berkovich indenter versus $f_{N2}$.

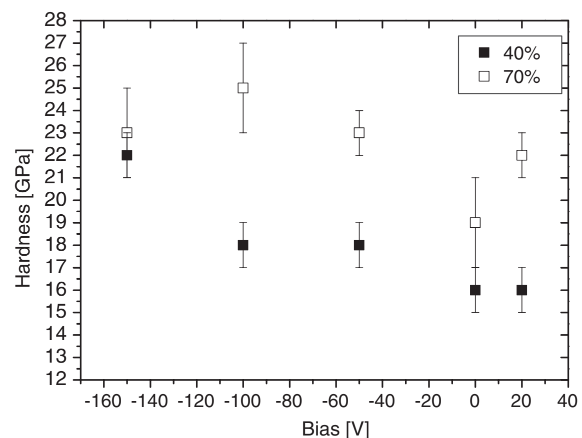


Fig. 10. Hardness of samples deposited at different bias and $f_{N2}$=40% (closed symbols) and $f_{N2}$=70% (open symbols).

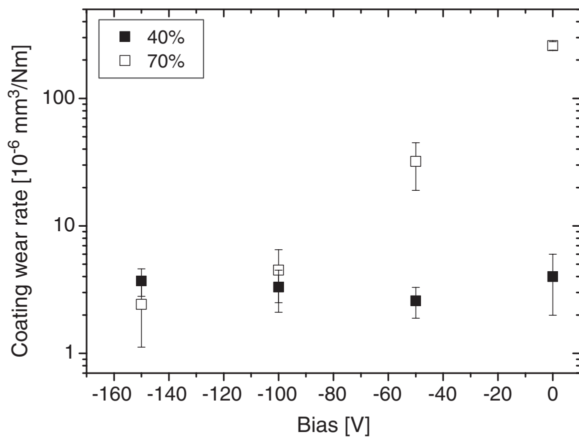


Fig. 11. Wear rate of samples deposited at different bias and $f_{N2}$ = 40% (closed symbols) and $f_{N2}$ = 70% (open symbols).

expected not only to reduce the hardness but also to provoke a higher plasticity, improving their toughness and wear resistance [31]. As it is known, in practical applications film toughness (ability to absorb deformation energy, both elastic and plastic) can be as important as hardness [32]. As a consequence, the lower wear coefficient of the films deposited at $f_{N2}$ = 40% and zero bias causes these samples to be less influenced by the hardness variation observed at higher negative bias (see Fig. 10). On the other hand, as the films deposited at $f_{N2}$ = 70% show a higher wear coefficient at zero bias, but they are more prone to further wear reduction induced by the hardness rise detected at increasing negative bias.

We have observed, in all the samples, a large dispersion of the sliding distance before the counterpart reaches the substrate. Consequently, the friction coefficient was measured in a range common to all the samples (1.25 m $\geq s \leq$ 12.5 m). Within this range, the friction coefficient ($\mu$) for $f_{N2}$ = 40% and 70% takes values between 0.40 and 0.48. For higher sliding distance (in some samples until 628 m, or 100,000 revolutions), a slight and monotonically increase of friction coefficient with sliding distance was observed. Similar results were obtained by van Essen et al. [33].

## 4. Conclusions

$CrN_x$ coatings have been deposited by reactive magnetron DC sputtering from a Cr target in a nitrogen atmosphere at increasing $N_2$ flows, while keeping the $Ar+N_2$ total flow constant (11 sccm). The crystalline phase sequence obtained with increasing $f_{N2}$ from 2% to 100% is Cr+N, $Cr+CrN_x$, Cr+CrN and $Cr_2N$, quite different to the results given by others researches who normally obtain CrN at the end of the sequence by changing $f_{N2}$ while keeping $f_{Ar}$ constant The nitrogen incorporation into the coating saturates at $f_{N2}$ = 40%, remaining constant at higher nitrogen flows. The saturation value defines two different regimes in the deposition process: below $f_{N2} \approx 40\%$, characterised by a mixture of phases, and above $f_{N2} \approx 40\%$, where pure $Cr_2N$ is obtained. The target poisoning effect has been studied monitoring the discharge voltage and has been found to occur between $f_{N2}$ = 35% and 40%. The application of bias has no effect on the phase formation but on the preferred crystal orientation and the residual tensions.

The hardness values without bias are around 20 GPa, with a maximum value of 21 GPa for $f_{N2}$ = 100% ($Cr_2N$ phase). The minimum value of hardness is at $f_{N2}$ = 40% where the phases CrN + Cr are presented. Applied bias show a strong influence on hardness, which increases with the negative bias up to 25 GPa for $f_{N2}$ = 70% and −100 V bias. In both nitrogen flows, $f_{N2}$ = 70% and 40%, the microstructure of the coatings changes from columnar to granular with increasing negative bias. In parallel, the coating wear rate decreases with increasing negative bias voltage for the $Cr_2N$ films, whereas in the CrN + Cr phases the wear coefficient remains practically constant, with lower values than in the former case. This has been explained as a consequence of plasticity caused by the presence of the Cr atoms in the films.

## References

[1] B. Navinsek, P. Panjan, I. Milosev, Thin Solid Films 281–282 (1997) 298.
[2] B. Liu, Corros. Sci. 43 (2001) 1953.
[3] M.A.M. Ibrahim, S.F. Korablov, M. Yoshimura, Corros. Sci. 44 (2002) 815.
[4] S.B. Sant, K.S. Gill, Surf. Coat. Technol. 68–69 (1994) 152.
[5] K. Baba, R. Hatata, Surf. Coat. Technol. 66 (1994) 368.
[6] Z.P. Huang, Y. Sun, T. Bell, Wear 173 (1994) 13.
[7] T. Sato, Y. Tada, M. Ozaki, K. Hoke, T. Besshi, Wear 178 (1994) 95.
[8] C. Rebholtz, H. Ziegele, A. Leyland, A. Matthews, Surf. Coat. Technol. 115 (1999) 222.
[9] C. Meunier, S. Vives, G. Bertrand, Surf. Coat. Technol. 107 (1998) 149.
[10] T. Hurkmans, D.B. Lewis, H. Paritong, J.S. Brooks, W.D Münz, Surf. Coat. Technol. 114 (1999) 52.
[11] Kyung H. Nam, Min J. Jung, Jeon G. Han, Surf. Coat. Technol. 131 (2000) 222.
[12] A. Barata, L. Cunha, C. Moura, Thin Solid Films 398–399 (2001) 501.
[13] G. Wei, A. Rar, J.A. Barnard, Thin Solid Films 398–399 (2001) 460.
[14] S.M. Aouadi, T.Z. Gorishnyy, D.M. Schultze, S.L. Rohde, Surf. Coat. Technol. 153 (2002) 1.
[15] Zenghu Han, Jiawan Tian, Qianxi Lai, Xiaojiang Yu, Geyang Li, Surf. Coat. Technol. 162 (2003) 189.
[16] P. Hones, N. Martin, M. Regula, F. Lévy, J. Phys., D. Appl. Phys. 36 (2003) 1023.
[17] D. Depla, J. Haemers, R. De Gryse, Plasma Sources Sci. Technol. (2002) 91.
[18] R. Mientus, K. Ellmer, Surf. Coat. Technol. 116–119 (1999) 1093.
[19] I. Safi, Surf. Coat. Technol. 127 (2003) 203.
[20] S. Berg, T. Nyberg, Thin Solid Films 476 (2005) 215.
[21] M.A. Auger, R. Gago, M. Fernández, O. Sánchez, J.M. Albella, Surf. Coat. Technol. 157 (2002) 26.
[22] P. Hones, R. Sanjines, F. Lévy, Surf. Coat. Technol. 94–95 (1997) 398.
[23] T.A. Delchar, Vacuum Physics and Techniques, Chapman and Hall, 1993, p. 93.
[24] J. Xu, H. Umehara, I. Kojima, Appl. Surf. Sci. 201 (2002) 208.
[25] Z. Han, J. Tian, Q. Lai, X. Yu, G. Li, Surf. Coat. Technol. 115 (1999) 222.
[26] L. Cunha, M. Andristschky, K. Pischow, Z. Wang, Thin Solid Films 355–356 (1999) 465.
[27] P.M. Fabis, Surf. Coat. Technol 52 (1992) 243.
[28] M. Berger, L. Karlsson, M. Larsson, S. Hogmark, Thin Solid Films 401 (2001) 179.
[29] G. Bertr, C. Savall, C. Meunier, Surf. Coat. Technol. 96 (1997) 323.
[30] ASTM G 99–95a.
[31] S. Zhang, D. Sun, Y. Fu, H. Du, Surf. Coat. Technol. 198 (2005) 2.
[32] A. Leyland, A. Matthews, Surf. Coat. Technol. 177–178 (2004) 317.
[33] P. van Essen, R. Hoy, J.-D. Kamminga, A.P. Ehiasarian, G.C.A.M. Jansen, Surf. Coat. Technol. (in press).